TECHNISCHE UNIVERSITÄT BERGAKADEMIE FREIBERG
The University of Resources. Since 1765.

Multiscale 3D stress field modelling for the URL 'Reiche Zeche' using a discontinuum model approach

MSc. Sebastian Rehde, Prof. Dr.-Ing. habil. Heinz Konietzky

EGU General Assembly 2020

Bundesministerium für Bildung und Forschung

Background and motivation

As part of the STIMTEC project we investigated the in situ stress field at the Reiche Zeche Underground Research Lab (URL) in Freiberg, Saxony. A multiscale 3D numerical analysis was performed using a discontinuous, anisotropic elastic approach incorporating stress data from literature. The model results were validated by hydrofrac stress measurements at the project test site. Stress data from a recent study gave reason to investigate the effect of an EDZ around the mine drifts.

Materials

The numerical analysis is based on 3D geological models developed on the basis of maps and digital data. These GIS-models were created with GOCAD.

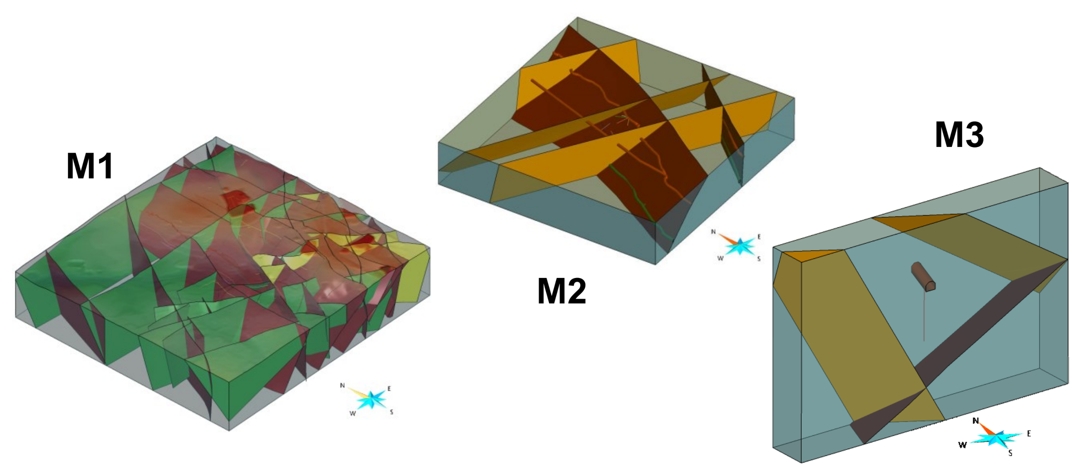

Fig. 1: a) Large scale model M1 (2500x2500x500 m) with 43 faults and mine drifts. Used to calculate stress tensors at small scale model boundary. b) Small scale model M2 (250x250x50 m) with 5 faults and mine drifts used to calculate in situ stress field at the investigation site. c) Slice model M3 (70x10x50 m) with 3 faults and mine drift used to investigate the influence of a potential EDZ around the drift. The test site is centred in the large and small scale models.

The regional stress field describes a strike-slip regime with a ratio of 1.2 : S_v : 0.7. The vertical stress is equal to the overburden and S_H is striking in NNW direction. Local stress field data from overcoring measurements [5] near the investigation area of the Stimtec project used for validation of M1 are listed in Table 1.

Tab 1.: Stress data from [5]

S_H [MPa]	S_v [MPa]	S_h [MPa]	α	γ
4.5	3.6	2.8	347°	0°

Mechanical parameters for the anisotropic, faulted, crystalline rock (Freiberger Graugneis) taken from cores and corrected for a geological strength index GSI=80 after [2] are listed in Table 2. We used a transversely isotropic, elastic constitutional law for a plane of isotropy dipping with 15° in southern direction. Faults were assigned the Mohr-Coulomb failure criterion and are able to undergo slip or tensile failure.

Tab 2.: Mechanical parameters of rock and faults from core tests.

Gneiss $_{GSI=80}$	ρ $[kg\,m^{-3}]$	E $[GPa]$	ν	G $[GPa]$	K $[GPa]$
$\parallel_{foliation}$	2700	52.8	0.2	43.9	20.3
$\perp_{foliation}$	2700	35.2	0.13	19.6	15.85

Faults	θ [°]	ψ [°]	k_n $[MPa/m]$	k_s $[MPa/m]$	c $[MPa]$	σ_t
	25	5	228.4	2284	0	0

Methods and results

For the numerical analysis we used the distinct element code 3DEC (Itasca). It allows representation of displacements along the numerous faults in the investigation area.
Stress boundary conditions corresponding to the regional stress field were applied to the large model, which then was validated by stress data from [5]. Because M2 is centred in M1, the boundary stress for M2 was taken directly from the results of M1. M2 was validated using the stress measurements performed in the injection borehole BH10 (slightly dipping north) and validation borehole BH17 (vertical) of the Stimtec project. Parameters and boundary conditions of M1 & M2 were variied to investigate their influence on the model results.

Large scale model M1

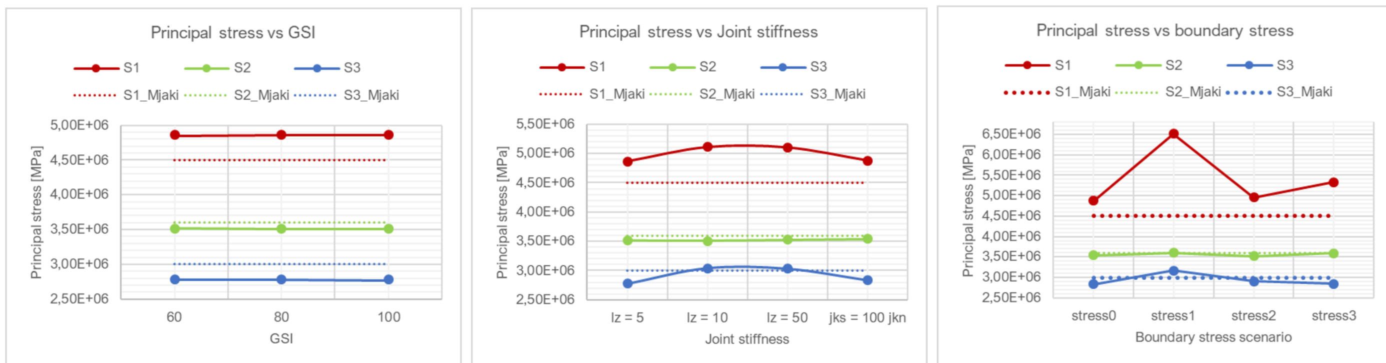

Fig. 2: Results for different model settings. Left: Results for GSI-values 60, 80 & 100. Centre: Results for different joint stiffnesses, with GSI=80. lz is a factor equal to smallest element edge and controls numerical stability via fault stiffness, based on [7]. We additionally investigated the results for jks = 100*jkn with lz = 5, which gave the best results for the large model. Right: Results for different initial and boundary stress conditions with GSI = 80 and jks = 100 jkn. S1,2,3_Mjaki are the stress data from [5].

Small scale model M2 – BH10 & BH17

The simulation procedure for model M2 contained several steps: (1) primary equilibrium for the virgin rock mass, (2) excavation of the drifts and (3) finally calculating the secondary equilibrium. The model results are verified by the data from BH10. Different boundary stress fields resulting from M1 were tested for model M2 (Fig. 3).
The data from validation borehole BH17 could not be reproduced with M2. The measurements showed a change in stress regime (SS to TF) with raised stress magnitudes for S_H and S_h.

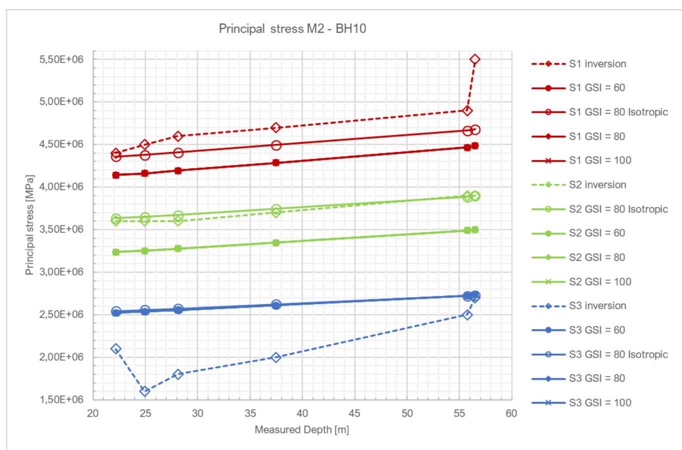

Fig. 3: Results for M2 in BH10. Principal stresses for different GSI-values and corresponding boundary stress fields from M1. Inversion data from project partners at RUB for BH10 measurements were used for validation. For better comparison with the inversion data, we calculated one model with isotropic elastic constitutional law.

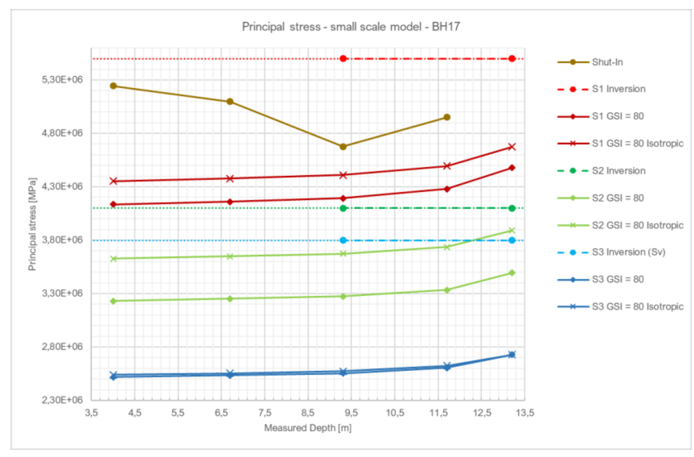

Fig. 4: Results for M2 in BH17. Inversion results of the measurements show a thrust faulting stress regime and strong increase of magnitude for horizontal principal stresses (1-2 MPa). Vertical stresses from inversion data and istropic M2 correspond well (S3 Inversion – cyan, S2 Isotropic - green) . However, M2 delivers a strike-slip regime for BH17.

Slice model M3 – EDZ

To investigate the local perturbation of the stress field measured in BH17, we introduced an excavation damage zone (EDZ $_1$), an excavation disturbance zone (EDZ $_2$) and a thickness to the prominent "Wilhelm Stehender" ore vein within the slice model M3 (see Fig.1). Assumed radii for EDZ $_1$ and EDZ $_2$ are $r_{EDZ_1} = 2{,}5 * r_{tunnel}$ and $r_{EDZ_1} = 5{,}5 * r_{tunnel}$ with $r_{tunnel} = 2m$ assumed Fault zone thickness $d_{FZ} = 2m$. BH17 is centred in M3. We developed five different model scenarios (Tab. 3) to study the effect of changes in formation modulus E_n or geometrical features (Fig. 5).

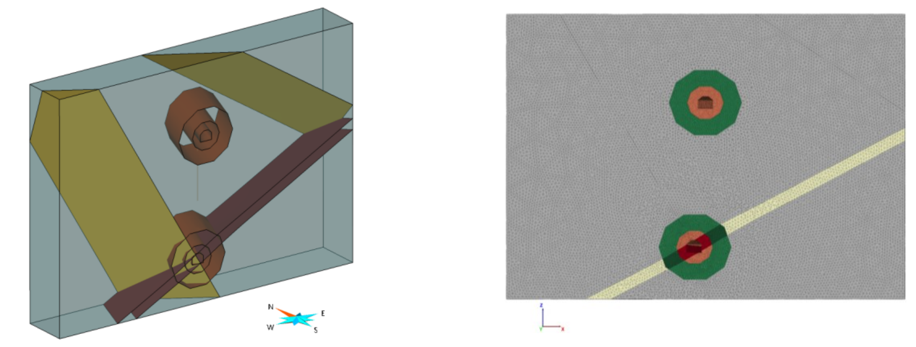

Fig. 5: Slice model with added features. Right: Geometry of scenario E (see Tab. 3). The idea was to investigate the effect of a potential drift on the lower mining level. The validation borehole BH17 has a length of 15 m and would end in the centre between both excavation levels. Grey: Host rock, Orange: Inner damage zone EDZ $_1$, Green: outer disturbance zone EDZ $_2$, Beige: Fault zone Wilhelm Stehender FZ, Red: Inner damage zone of fault zone FZ_EDZ $_1$, Darkgreen: Outer disturbance zone of fault zone FZ_EDZ $_2$.

Tab. 3: Model scenarios for M3.

Scenarios	f_{EDZ_1}	f_{EDZ_2}	f_{FZ}	$f_{FZ_{EDZ_1}}$	$f_{FZ_{EDZ_2}}$	Geological features	Reference
A	0.3	0.5	0.05			Sohle 1 with EDZs	[6]
B	0.5	0.8	0.3			Sohle 1 with EDZs	[1]
C	0.25	0.5	0.1			Sohle 1 with EDZs	[4]
D	0.3	0.5	0.05			Sohle 1 with EDZs bedding planes	[6]
E	0.3	0.5	0.05	0.03	0.025	Sohle 1 with EDZs Sohle 2 with EDZs	[6]

$$E_n = f_n \cdot E_{host\,rock} \quad (1)$$

Scenarios A-C, with same geological features, are used to examine the influence of different EDZ and FZ formation moduli. Equation 1 shows how elastic properties were reduced according to literature ([1], [4], [6]).
Scenario D is used to investigate effects of bedding planes. Therefore, two discontinuities parallel to the bedding plane orientation were added to the model. They strike through EDZ $_2$ of the tunnel. With scenario E we examined the impact of a potential second drift and its associated EDZs 25 m below our drift (Fig. 5). The modelling procedure for M3 considered a primary equilibrium with no drifts or EDZs. For the secondary equlibrium the drift elements were deleted and Young's moduli of all EDZ elements were weakened as listed in Tab. 3. The aim was to simulate the process of excavation and subsequent damaging of the rock surrounding the mine drifts. The drifts were excavated by drill and blast more than hundred years ago.

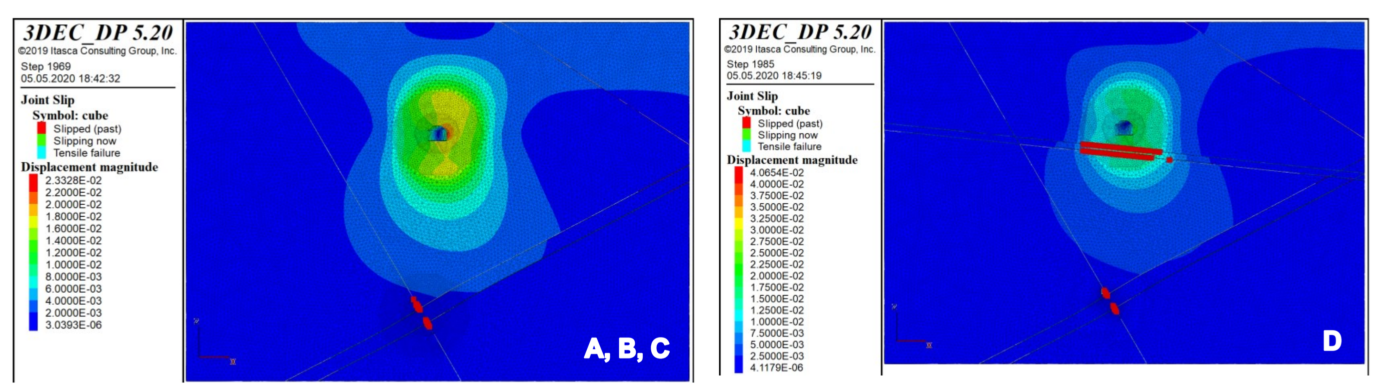

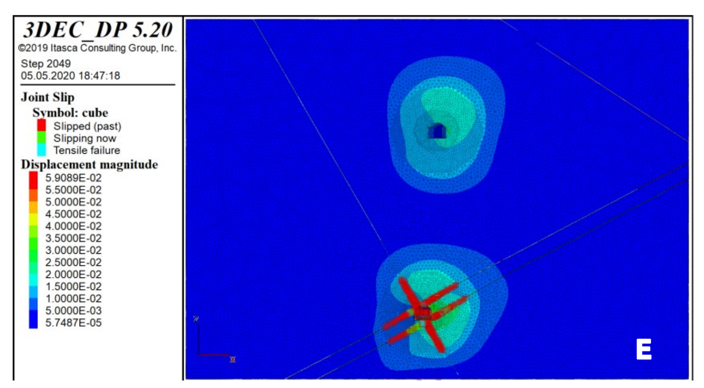

Fig. 6: Displacement magnitudes for Scenarios A-E. Scenarios A,B,C show the smallest displacements but the distribution of displacements shows the widest spread. Scenario D lets assume that the bedding plane contains the spread of displacements. Scenario E shows least displacements spread. For all scenarios positive and negative maximum displacements appear at the tunnel contour and along the block tips at intersections of discontinuities.

Interpretation of M3 results

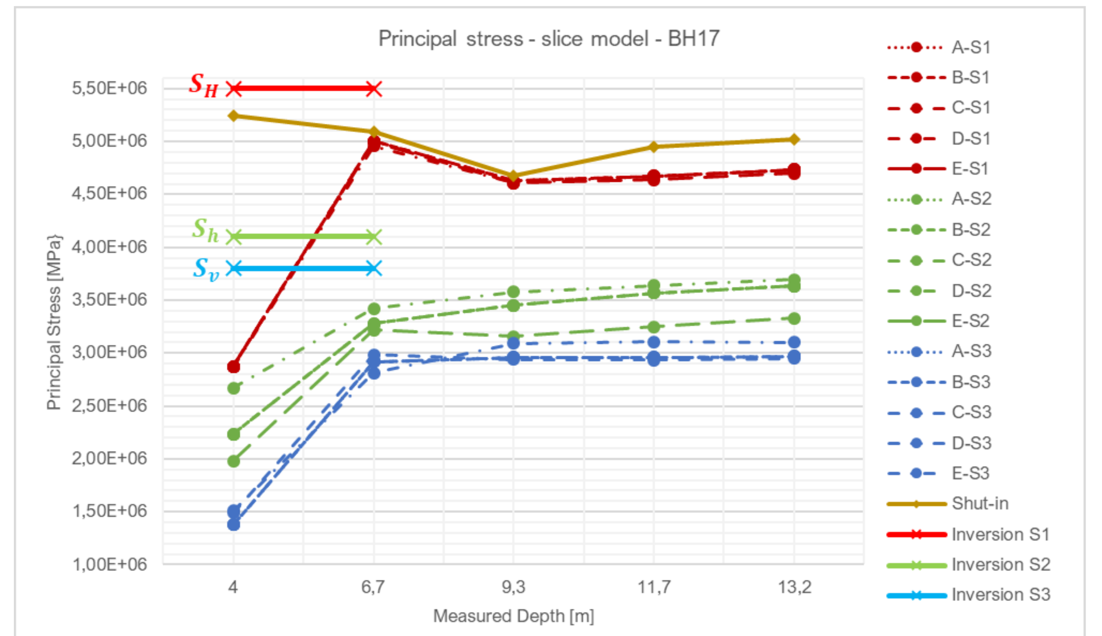

Fig. 7: Resulting principal stresses for BH17 from model M3. Horizontal principal stresses do not differ much between scenarios. Stress regime is strike slip for M3. Solid lines represent TF stressfield magnitudes from Inversion results.

For the chosen Young's moduli, model M3 did not provide satisfying results. It was only possible to obtain a change in stress regime from strike slip to thrust fault for extremely low Young's moduli, which are not realistic. However, the results would still not show the strong increase of S_h.
This suggests that the chosen model approach is not suitable to elucidate the observations from BH17 numerically. The damages from drift excavation are not well represented by the proposed approach. Thus, local stress field perturbations cannot be duplicated by this model, but the overall stress field is well reproduced.

Outlook

Future work should include additional measurements in-situ and other modelling approaches, for instance by considering other constitutive models. The EDZ may be better represented by a DFN or complex elasto-plastic constitutive models with strain softening. Another approach could consider local inhomogeneities of the rock mass by assuming statistical distribution of properties. Finally, also the assumption of local stress variations (locked-in stresses) created during the geological process should be considered. Best would be to lay emphasis on the influence of the bedding planes as a discontinuity. As shown in Fig. 6, the bedding plane has a provable influence on the displacements in the rock after excavation of the tunnels. Yet, model M3, scenario D can only show the function of the method as there are only two bedding planes in the model, with much larger spacing than in reality.

References:
1) Carpenter, B. M., H. Kitajima, R. Sutherland, J. Townend, V. G. Toy, and D. M. Saffer (2014), Hydraulic and acoustic properties of the active Alpine Fault, New Zealand: Laboratory measurements on DFDP-1 drill core, Earth Planet. Sci. Lett., 390,45–51, doi:10.1016/j.epsl.2013.12.023.
2) Hoek, E.; Brown, E.T.The Hoek–Brown failure criterion and GSI – 2018 edition, Journal of Rock Mechanics and Geotechnical Engineering, Volume 11, Issue 3, 2019, Pages 445-463, ISSN 1674-7755, https://doi.org/10.1016/j.jrmge.2018.08.001.
3) Jaeger, John Conrad; Cook, Neville G. W.; Zimmerman, Robert W. (2011): Fundamentals of rock mechanics. 4. ed.
4) Jeanne, P., Y. Guglielmi, J. Rutqvist, C. Nussbaum, and J. Birkholzer (2017), Field characterization of elastic properties across a fault zone reactivated by fluid injection, J. Geophys. Res. Solid Earth, 122, 6583–6598, doi:10.1002/2017JB014384.
5) Mjakischew, V. "Untersuchung des Gebirgsspannungszustandes im Südostteil der DDR". In: Freiberger Forschungshefte - Beiträge zur Gebirgsmechanik 1987.A740 (1987), pp. 7–48.
6) Villeneuve, M.C., Heap, M.J., Kushnir, A.R.L. et al. Estimating in situ rock mass strength and elastic modulus of granite from the Soultz-sous-Forêts geothermal reservoir (France). Geotherm Energy 6, 11 (2018). https://doi.org/10.1186/s40517-018-0096-1
7) Zeeb, C.; Herbst, M.; Damjanac, B.; Wolgast, D.; Konietzky, H., „Coupled HM simulations in 3DEC – Tips and Tricks" – internal report at Institute for rock mechanics, TU Freiberg, 2014

Software used: 3DEC, GRIDDLE by ITASCA, RHINO 5, SKUA/GOCAD by Paradigm, Matlab

MSc. Sebastian Rehde, Prof. Dr.-Ing. habil. Heinz Konietzky
TU Bergakademie Freiberg | Institut für Geotechnik | Professur für Felsmechanik | Gustav-Zeuner-Str. 1| 09599 Freiberg | Telefonnummer: 03731 / 39-3545 | sebastian.rehde@ifgt.tu-freiberg.de